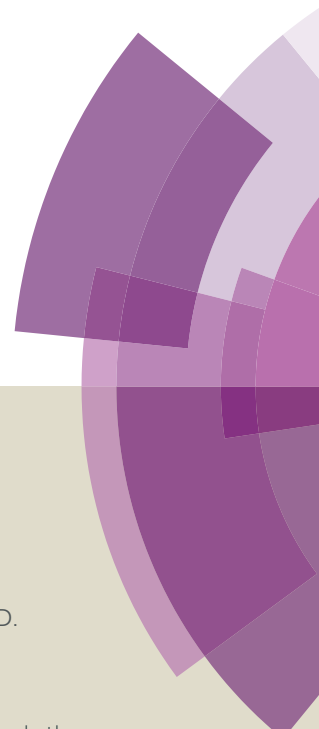


Journal of Materials Chemistry A

Accepted Manuscript



This article can be cited before page numbers have been issued, to do this please use: S. Li, H. Wang, D. Li, X. Zhang, Y. Wang, J. Xie, J. Wang, Y. Tian, W. Ni and Y. Xie, *J. Mater. Chem. A*, 2016, DOI: 10.1039/C6TA07545B.



This is an *Accepted Manuscript*, which has been through the Royal Society of Chemistry peer review process and has been accepted for publication.

Accepted Manuscripts are published online shortly after acceptance, before technical editing, formatting and proof reading. Using this free service, authors can make their results available to the community, in citable form, before we publish the edited article. We will replace this *Accepted Manuscript* with the edited and formatted *Advance Article* as soon as it is available.

You can find more information about *Accepted Manuscripts* in the [Information for Authors](#).

Please note that technical editing may introduce minor changes to the text and/or graphics, which may alter content. The journal's standard [Terms & Conditions](#) and the [Ethical guidelines](#) still apply. In no event shall the Royal Society of Chemistry be held responsible for any errors or omissions in this *Accepted Manuscript* or any consequences arising from the use of any information it contains.

Siloxene nanosheet: A metal-free semiconductor for water splitting

Shuang Li,^a Hui Wang,^a Dandan Li,^b Xiaodong Zhang,^{*a} Yufeng Wang,^a Junfeng Xie,^a Jingyao Wang,^a Yupeng Tian,^b Wenxiu Ni^c and Yi Xie^{*a}

Received 00th January 20xx,
Accepted 00th January 20xx

DOI: 10.1039/x0xx00000x

www.rsc.org/

Exploring efficient semiconductors for water splitting to produce hydrogen is considered as one of the most promising approach to solving the world energy crisis. Herein, for the first time, we highlight that the metal-free siloxene nanosheet can serve as a photocatalyst for efficient water splitting without the addition of any cocatalyst or sacrificial agent.

The growing global energy demand and environmental pollution issues have led to the urgent need for renewable and efficient green energy sources. In this respect, hydrogen, a sustainable and clean energy source has been considered as a promising candidate for replacing traditional fossil fuels.¹⁻² The use of semiconductor with solar energy to split water is a highly controlled approach to convert sunlight into clean and storable hydrogen.³⁻⁶ Hence, the development of the efficient semiconductors for hydrogen evolution is greatly demanded. In recent years, metal-free semiconductors such as g-C₃N₄, red phosphorus, sulfur have been actively pursued, for their cost-effective and environmental friendly.⁷⁻⁹ Despite progresses have been made, the metal-free semiconductors suffer from low hydrogen evolution ability without the adding of co-catalysts or sacrificial agents, which greatly hampered their extensive applications. In that case, it is of great significance to seek new metal-free semiconductors with the merits of commercially available and excellent intrinsic hydrogen generation performances.

Bear this in mind, we paid our attentions to the silicon-based material, whose excellent optical properties make them to be potential candidates for photocatalysts.¹⁰⁻¹⁵ Although a variety of functional silicon-based materials have been identified, their applications are mainly confined to dye degradation, while neglected success was achieved in water

splitting for the improper band structures.¹⁶⁻²¹ As a direct bandgap semiconductor, siloxene (Si₆H₆O₃) possesses a two-dimensional structural configuration, which is formed by an array of linear Si chains interconnected with oxygen bridges and terminated by hydrogen (Fig. 1a, 1b). Herein, the electronic structure of the single-layered siloxene was studied by the time-dependent density functional theory (TD-DFT). Similar to graphene, the siloxene possesses π -conjugated electronic structure. As shown in Fig. 1c, 1d, the HOMO and LUMO orbitals of the siloxene are well delocalized over the π -conjugated skeletons, which are helpful for the molecular charge-transfer transition under light irradiation. Because the photocatalytic reaction is strongly correlated with the molecular charge-transfer transition, the siloxene would be used for photocatalytic reaction. In addition, the calculated total energy of single-layered siloxene nanosheets is about -160.72 KeV, which is negative enough for the stabilization of

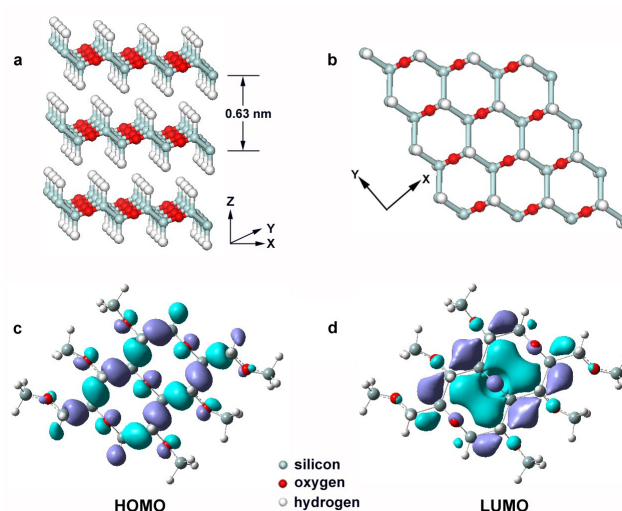


Fig. 1 (a) Side view of the layer structure of siloxene. (b) Top-view of the siloxene. (c) and (d) HOMO and LUMO orbitals of the single-layered siloxene, respectively.

^a Hefei National Laboratory for Physical Sciences at the Microscale, Collaborative Innovation Center of Chemistry for Energy Materials, University of Science and Technology of China, Hefei, Anhui, 230026, P. R. China.

E-mail: zhxid@ustc.edu.cn, yxie@ustc.edu.cn

^b Department of Chemistry, Anhui University, Hefei, Anhui, 230039, P. R. China.

^c Department of Chemistry, Shantou University, Shantou, 515063, P. R. China.

† Electronic Supplementary Information (ESI) available: See DOI: 10.1039/x0xx00000x

the siloxene molecules. Given its unique π -conjugated electronic structure, the siloxene may be a new metal-free photocatalyst for hydrogen evolution. Herein, for the first time, we show that siloxene nanosheet can generate hydrogen by photocatalytic water splitting, rendering it to be a new semiconductor-based photocatalyst.

In this study, siloxene nanosheets were prepared by a topotactical reaction from the Zintl Phase CaSi_2 , a layered material with Si corrugated (111) planes linked by Ca ions. As schematically illustrated in Fig. 2a, the black CaSi_2 would transform into a yellow-green solid during the topotactical reaction. The morphology of the as-obtained product was studied by the transmission electron microscopy (TEM) image. As displayed in Fig. 2b, the free-standing nanosheets with lateral size of about a few hundred nanometers can be seen, and the near transparency of the nanosheets indicates their ultrathin nature. The thickness of the nanosheets was measured to be about 4.8 nm by the atomic force microscopy (AFM) (Fig. S1[†]), which is consistent with about eight individual siloxene layers. Elemental mapping analysis was carried out to investigate the chemical composition of the product firstly (Fig. 2c), from which the homogeneous distribution of silicon and oxygen can be identified across the whole nanosheet. In addition, X-ray photoelectron spectroscopy (XPS) and X-ray absorption near edge structure (XANES) spectroscopy were performed to investigate the configuration of the as-prepared siloxene nanosheets (Fig. S2[†] and S3[†]), giving direct evidence that the Si chains in the nanosheets were interconnected with oxygen bridges and terminated by hydrogen. Moreover, Raman spectrum of the product in Fig. 2d clearly demonstrates the presence of Si-Si vibrations (380 and 515 cm^{-1}), Si-O vibrations (495 cm^{-1}) and Si-H vibrations (635 and 730 cm^{-1}) in the structure, further confirming the successful preparation of siloxene nanosheets with linear Si chains.

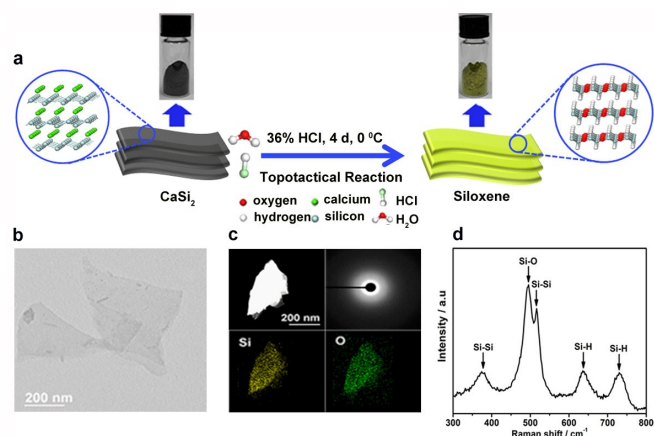


Fig. 2 (a) Schematic illustration of the strategy for the preparation of siloxene nanosheets. (b) TEM image of the ultrathin siloxene nanosheets. (c) EDS mapping images of the as-prepared siloxene nanosheets. The corresponding selected area electron diffraction (SAED) pattern reveals its amorphous

character. (d) Raman spectrum of the as-prepared siloxene nanosheets.

DOI: 10.1039/C6TA07545B

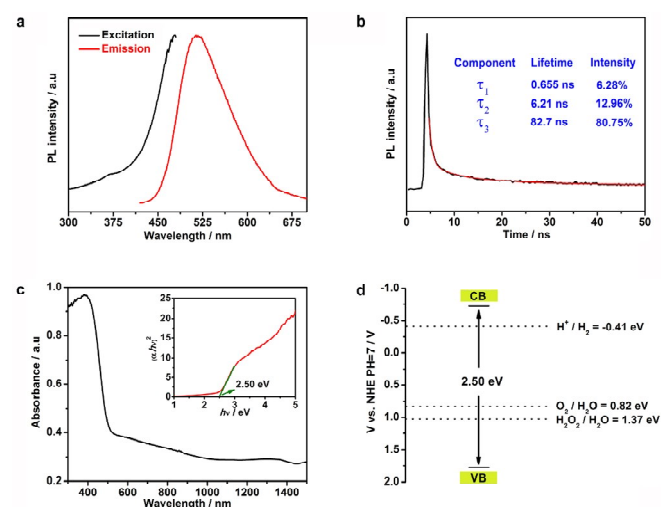


Fig.3 (a) PL excitation and emission spectra of siloxene nanosheets. Emission spectrum was excited at 400 nm. (b) Time-resolved PL spectrum monitored at 515 nm under 400 nm excitation at 298 K for siloxene nanosheets. (c) UV-vis absorption spectrum of siloxene nanosheets. Inset: the corresponding bandgap. (d) Band structure of siloxene nanosheets according to the bandgap and flat-band potential (-0.92 V).

The optical properties of siloxene nanosheets were studied by the combined analyses of the photoluminescence (PL) spectrum and UV-Vis absorption spectrum. The excitation spectrum of siloxene nanosheets was shown in Fig. 3a, from which we choose 400 nm to excite the PL spectrum, emitting fluorescence located at about 515 nm. The average lifetime of PL spectrum monitored at 515 nm is 67.6 ns (Fig. 3b), suggesting the electrons and holes that generated by siloxene can be separated with each other at a relatively long time for photocatalysis. As shown in Fig. 3c, the optical absorption spectrum of the as-prepared siloxene nanosheets shows an absorption onset at ca. 496 nm, from which the band gap was determined to be 2.50 eV. To go further, the conduction band of the as-obtained nanosheets was studied by Mott-Schottky analysis. As shown in Fig. S4[†], the flat-band potential was estimated to be -0.92 V, and the positive slope of this linear plot suggests the n-type character of the siloxene nanosheet. Based on those, the band structure of the siloxene nanosheet was summarized in Fig. 3d with the edge position of the conduction band (CB) locating above the hydrogen-evolution potential and the valence band (VB) below the oxidation level for H_2O to H_2O_2 or O_2 , indicating siloxene nanosheets satisfy the necessary requirements for water splitting. These results provide strong evidence that siloxene nanosheets have the potential to function as a photocatalyst for overall water splitting.

The photocatalytic activity of the siloxene nanosheet was evaluated by detecting its hydrogen evolution in water without the addition of any sacrificial reagent or cocatalyst. As shown

in curve (i) of Fig. 4a, the siloxene nanosheet can generate large amount of hydrogen up to $49.38 \text{ mmol g}^{-1}$ at initial 12 hours under simulated sunlight. These results indicate that siloxene

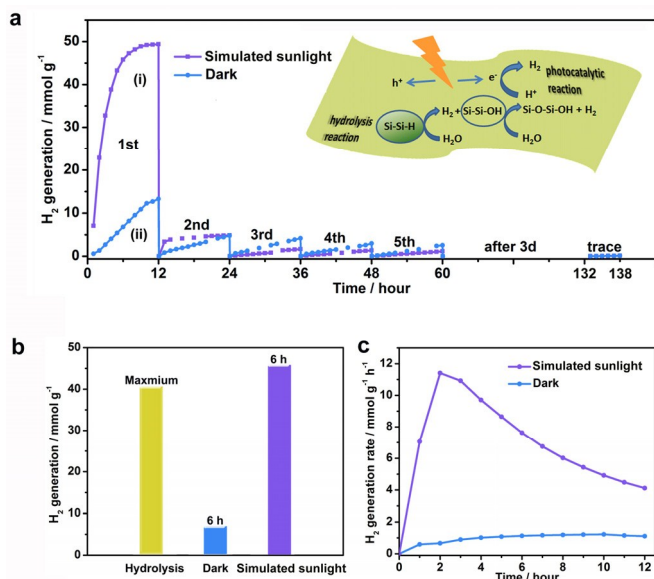


Fig. 4 (a) Time-dependent hydrogen evolution from siloxene aqueous solution at room temperature under different conditions: (i) under simulated sunlight and (ii) in the dark. Inset: the dual effect of hydrolysis reaction and photocatalytic reaction for hydrogen generation on light illumination. (b) Comparison of hydrogen evolution amount for different samples: theoretical maximum amount released by hydrolysis, the total amount at initial 6 hours generated in the dark and under simulated sunlight, respectively. (c) Comparison of hydrogen evolution rate in the first run for siloxene nanosheets in the dark and under simulated sunlight.

nanosheet is an efficient metal-free photocatalyst for solar-driven hydrogen evolution. Furthermore, the reaction was allowed to proceed initially for 60 consecutive hours with intermittent evacuation every 12 hours under simulated sunlight irradiation. It is found that, the amount of generated hydrogen was decreased by one order of magnitude after the first initial 12 hours, which was further decreased as time goes by. And only trace amount of hydrogen could be observed after reaction for 138 hours. The dramatically decreased hydrogen evolution indicates the unstable of the siloxene nanosheets in water. In order to study this issue, the same experiments were also recorded in the dark. As shown in curve (ii) of Fig. 4a, it is interesting that the siloxene nanosheets can release hydrogen even without light irradiation, which should be produced via hydrolysis process. That is the reason why the siloxene nanosheets become deactivated in photocatalytic activity with the increasing of time for light irradiation. Herein, the theoretically maximum amount of hydrogen can reach up to 40.54 mmol per gram siloxene nanosheets by hydrolysis (see supplementary text S2). As shown in Fig. 4b, the amount of hydrogen evolved after 6 hours for irradiation already reached 45.8 mmol g^{-1} , which is 1.13 times higher than that of

the theoretical maximum released by hydrolysis, and 6.76 times higher than that in the dark of about 6.78 mmol g^{-1} . These results clearly demonstrate that the existence of photocatalytic activities of siloxene nanosheets for hydrogen generation.

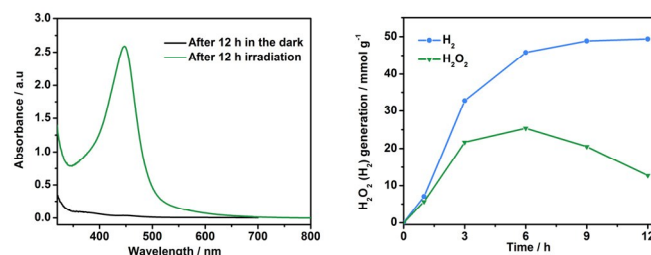


Fig. 5 (a) H₂O₂ generation from water using siloxene nanosheets after reaction for 12 h under simulated sunlight and in the dark. (b) A time course of H₂O₂ and H₂ generation from water under simulated sunlight by siloxene nanosheets.

As shown in Fig. 4c, under light irradiation, siloxene nanosheet possesses a maximum hydrogen generation rate of $11.4 \text{ mmol g}^{-1} \text{ h}^{-1}$, which is 17.2 times higher than that in the dark, suggesting the superior photocatalytic hydrogen evolution activity. Of note, this value is 393.1 times higher than that of the commercial Si with hydrogen evolution rate of $0.029 \text{ mmol g}^{-1} \text{ h}^{-1}$; 28.5 times higher than that of mesoporous crystalline Si of $0.4 \text{ mmol g}^{-1} \text{ h}^{-1}$.²² In addition, the maximum hydrogen generation rate of siloxene nanosheet is much higher than that of graphitic-C₃N₄.⁵ These results clearly indicate siloxene nanosheet to be a promising new metal-free photocatalyst for hydrogen generation.

In order to fully understanding the water splitting process of siloxene nanosheets, the mechanism for the photocatalytic hydrogen evolution was studied. During light irradiation, the siloxene can only generate hydrogen, without any oxygen. We deduced that the difficulty in O₂ generation may be attributed to the kinetically competitive reactions, such as a two-electron water oxidation process to hydrogen peroxide (H₂O₂) (see supplementary text S3). In that case, we check the products of water oxidation in the reaction system by a special peroxides indicator o-tolidine and monitored the absorption peak of o-tolidine at 447 nm using UV-Vis spectroscopy.²³⁻²⁶ As shown in Fig. 5a, the absorption peak at 447 nm in the UV-Vis spectrum is distinctly observed in the reaction system after irradiation for 12 hours, while no typical absorption peak is observed in the dark, suggesting the generation of H₂O₂ under light irradiation and the photocatalytic water splitting of siloxene nanosheets should undergoing a two-electron pathway. The total H₂O₂ production was measured up to 12.75 mmol per gram of siloxene nanosheet, which is calculated by a calibrated curve and fitting equation of H₂O₂ concentration with the absorbance at 447 nm (see Fig. S6†). Fig. 5b clearly shows the time-dependent H₂ and H₂O₂ generation of siloxene nanosheets from water under simulated sunlight. It can be seen that the amount of H₂O₂ greatly increased at the initial stage, while decreased after irradiation for 6 hours. This result implies that a decomposition reaction of H₂O₂ may take place

during the photocatalytic process. Detailed analysis (see supplementary text S4, Fig. S7† and S8†) shows that a portion of the generated H₂O₂ molecules decomposed to hydroxyl radical, thus, it would be expected that the actual amount of H₂O₂ generation via two-electron water oxidation process is larger than that of the estimated one.

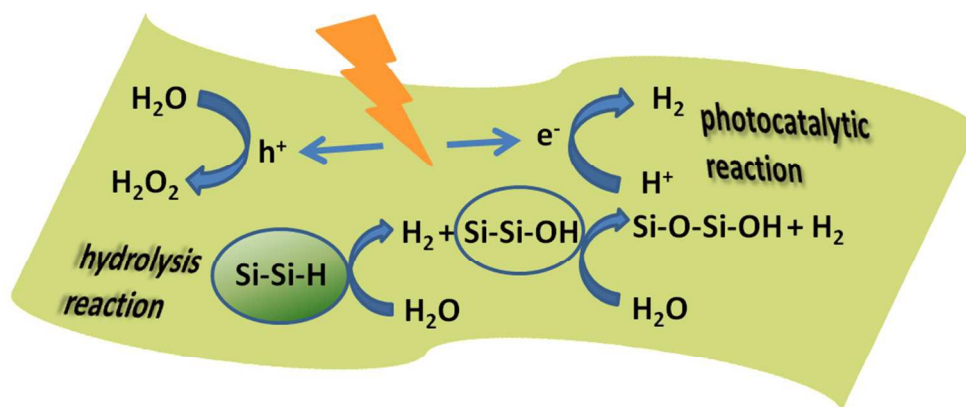
In conclusion, we have for the first time experimentally demonstrated the siloxene nanosheet to be a metal-free semiconductor for photocatalytic water splitting. With the merits of unique electronic structure and suitable bandgap, siloxene nanosheet can generate hydrogen and hydrogen peroxide via a two-electron pathway under light irradiation without the addition of any cocatalyst or sacrificial agent. Although siloxene nanosheet is unstable in water, siloxene exhibits excellent photocatalytic activity for hydrogen generation. For example, it can generate 45.8 mmol g⁻¹ of hydrogen at the first 6 hours under simulated sunlight, which is 1.13 times higher than that the theoretical maximum amount released by hydrolysis, and 6.76 times higher than that in darkness. Moreover, the maximum rate of hydrogen generation can up to 11.4 mol g⁻¹ h⁻¹, rendering the siloxene nanosheet to be a promising semiconductor for water splitting. We believe that this study can provide a new insight into the study of low-dimensional silicon-based functional materials.

Acknowledgements

This work was supported by the National Basic Research Program of China (2015CB932302), National Natural Science Foundation of China (U1532265, U1632149, 21331005, 11321503, 21401181, 91422303) and Fundamental Research Funds for the Central University (WK2060190027, WK2340000063), the Key Laboratory of Neutron Physics (CAEP, 2014DB01) and Research Grant of the Hefei Science Center of CAS (2015HSC-UE006, 2015HSC-UP015).

Notes and references

- M. S. Dresselhaus and I. L. Thomas, *Nature*, 2001, **414**, 332-337.
- J. A. Turner, *Science*, 2004, **305**, 972-974.
- X. Chen, S. Shen, L. Guo and S. S. Mao, *Chem. Rev.*, 2010, **110**, 6503-6570.
- Y. Tachibana, L. Vayssieres and J. R. Durrant, *Nat. Photon.*, 2012, **6**, 511-518.
- X. Wang, D. Liu, S. Song and H. Zhang, *J. Am. Chem. Soc.*, 2013, **135**, 15864-15872.
- X. Wang, Y. Zhang, S. Song, X. Yang, Z. Wang, R. Jin and H. Zhang, *Angew. Chem. Int. Ed.*, 2016, **55**, 4542-4546.
- X. Wang, K. Maeda, A. Thomas, K. Takanebe, G. Xin, J. M. Carlsson, K. Domen and M. Antonietti, *Nat. Mater.*, 2009, **8**, 76-80.
- F. Wang, W. K. H. Ng, C.Y. Jimmy, H. Zhu, C. Li, H. Zhu, L. Zhang, Z. Liu and Q. Li, *Appl. Catal., B*, 2012, **111-112**, 409-414.
- G. Liu, P. Niu, L. Yin and H. M. Cheng, *J. Am. Chem. Soc.*, 2012, **134**, 9070-9073.
- Z. Kang, C. H. A. Tsang, Z. Zhang, M. Zhang, N. B. Wong, J. A. Zapien, Y. Shan and S. T. Lee, *J. Am. Chem. Soc.*, 2007, **129**, 5326-5327.
- Y. Sugiyama, H. Okamoto, T. Mitsuoka, T. Morikawa, K. Nakanishi, T. Ohta and H. Nakano, *J. Am. Chem. Soc.*, 2010, **132**, 5946-5947.
- S. W. Kim, J. Lee, J. H. Sung, D. Seo, I. Kim, M. H. Jo, B. W. Kwon, W. K. Choi, and H. Choi, *ACS Nano*, 2014, **8**, 6556-6562.
- B. Tian, T. J. Kempa and C. M. Lieber, *Chem. Soc. Rev.*, 2009, **38**, 16-24.
- M. D. Kelzenberg, S. W. Boettcher, J. A. Petykiewicz, D. B. T. Evans, M. C. Putnam, E. L. Warren, J. M. Surgeon, R. M. Briggs, N. S. Lewis and H. A. Atwater, *Nat. Mater.*, 2010, **9**, 239-244.
- Y. Lin, C. Battaglia, M. Boccard, M. Hettick, Z. Yu, C. Ballif, J. W. Ager and A. Javey, *Nano Lett.*, 2013, **13**, 5615-5618.
- Z. Kang, C. H. A. Tsang, N. B. Wong, Z. Zhang and S. T. Lee, *J. Am. Chem. Soc.*, 2007, **129**, 12090-12091.
- M. Shao, L. Cheng, X. Zhang, D. D. Ma and S. T. Lee, *J. Am. Chem. Soc.*, 2009, **131**, 17738-17739.
- F. Y. Wang, Q. D. Yang, G. Xu, N. Y. Lei, Y. K. Tsang, N. B. Wong and J. C. Ho, *Nanoscale*, 2011, **3**, 3269-3276.
- N. Megouda, Y. Cofinier, S. Szunerits, T. Hadjersi, O. Elkechai and R. Boukherroub, *Chem. Commun*, 2011, **47**, 991-993.
- R. Q. Zhang, X. M. Liu, Z. Wen and Q. Jiang, *J. Phys. Chem. C.*, 2011, **115**, 3425-3428.
- D. Liu, L. Li, Y. Gao, C. Wang, J. Jiang and Y. Xiong, *Angew. Chem. Int. Ed.*, 2015, **54**, 2980-2985.
- F. Dai, J. Zai, R. Yi, M. L. Gordin, H. Sohn, S. Chen and D. Wang, *Nat. Chem.*, 2014, **5**, 3605-3615.
- D. Duonghong and M. Gratzel, *J. Chem. Soc., Chem. Commun.*, 1984, **1073**, 1597-1599.
- J. Kimi and M. Gratzel, *J. Mol. Catal.*, 1987, **39**, 63-70.
- O. C. Compton and F. E. Osterloh, *J. Phys. Chem. C*, 2009, **113**, 479-485.
- J. Liu, Y. Zhang, L. Lu, G. Wu and W. Chen, *Chem. Commun.*, 2012, **48**, 8826-8828.



186x89mm (150 x 150 DPI)